Int J Hum Genet, 18(2): 129-136 (2018)
DOI: 10.31901/24566330.2018/18.2.696

Revealing Dysregulated Modules and Genes for Postmenopausal Osteoporosis Based on Module Inference and Attract Method

Liang Ma[1], Wei-Guo Wang[1] and Xiao-Li Zhang[2]

[1]Department of Orthopaedics, Shandong Provincial Hospital of Traditional Chinese Medicine, Jinan, 250011, Shandong Province, China
[2]Department of Endocrinology, Shandong Provincial Hospital of Traditional Chinese Medicine, Jinan, 250011, Shandong Province, China

KEYWORDS Protein-Protein Interaction Network. Dysregulated Genes. Attract. Biomarkers. Treatment

ABSTRACT Postmenopausal osteoporosis (PO) imposes a significant burden on the individual and society. This work aimed to investigate dysregulated modules and genes for PO. Firstly, protein-protein interaction (PPI) data were prepared for the Retrieval of Interacting Genes/Proteins (STRING) database and gene expression data. Subsequently, attracted modules were explored from PPI networks by clique-merging algorithm and module correlation density (MCD) analyses. Ultimately, dysregulated modules between PO and normal were determined, and genes in the dysregulated modules were defined. A total of 7,953 genes and 48,778 interactions were collected for PPI data. Module 1 and Module 2 were identified for PO, and the two modules also detected as dysregulated modules. Module 1 included 6 dysregulated genes, while Module 2 with 7 dysregulated genes. The dysregulated modules and genes might be potential biomarkers for prevention and treatment of PO, which give new insights for revealing molecular mechanism of PO.

INTRODUCTION

Postmenopausal osteoporosis (PO) is defined as a silent skeletal disorder that characterized by compromised bone strength predisposing to an increased risk of fracture (Ozsoy et al. 2017). To the best of the researchers' knowledge, it is suggested to directly result from a lack of endogenous oestrogen in menopausal females (Manocha et al. 2017). Specifically, hormonal changes, which occur throughout perimenopause and the immediate postmenopausal years, stimulate the receptor activator of nuclear factor-κβ (RANK) and its ligand (RANKL) production (both directly and indirectly), leading to accelerated bone loss (Stuss et al. 2013). Low bone mass density and fracture are two major manifestations of PO patients clinically, and even vertebral compression fractures may happen during routine daily activities without a specific fall or injury (Unni et al. 2015). In consequence, PO imposes a significant burden on both the individual and society. Fortunately, it can be prevented, diagnosed, and treated before fractures occur (Cosman et al. 2014).

Address for correspondence:
Xiao-Li Zhang
Department of Endocrinology,
Shandong Provincial Hospital of Traditional Chinese Medicine,
No. 42 on Wenhua West Road,
LiXia District, Jinan, 250011,
Shandong Province, China
Telephone & Fax: 86-0531-68617953
E-mail: xiaolizhangsd@163.com

The most commonly used drugs approved to treat PO are the antiresorptive medications to inhibit osteoclastic bone resorption, such as the nitrogen-containing bisphosphonates and RANKL inhibitor denosumab, whereas they do so by different cellular and molecular mechanisms (Delmas 2008; Tsai et al. 2013). The other effective treatments comprise conventional radiography, dual-energy X-ray and chemical biomarker which a useful tool in detecting bone degradation (Orwoll et al. 2013). In addition, with the rapid development of high throughput techniques, it has been applied to explore diagnostic potential signatures and biological processes of human diseases (Jordán et al. 2012). For example, miR-133a in circulating monocytes was defined as a potential biomarker for PO (Wang et al. 2012). Despite certain number of biomarkers are uncovered, it is still far from understanding molecular mechanisms happening inside PO patients (Svedbom et al. 2014).

Traditionally, biomarkers are usually obtained by identifying the most significant differentially expressed genes (DEGs) between disease samples and normal controls (Liu et al. 2012a). Nevertheless, genes are not only encoded as individual genes or proteins, but also interacted with others to form interactions (Vinayagam et al. 2014). Network concept has been proposed for

purpose of solving this problem. Network-based approach is capable of extracting informative and significant genes and sub-networks dependent on molecular networks, for instance, protein-protein interaction (PPI) network (Liu et al. 2012b). Meanwhile, it offers a quantifiable description of the networks that characterize the complex interactions and the intricate interwoven relationships that govern cellular functions, among those tissues and disease related genes to explain the molecular processes during disease development and progression (Sun et al. 2013).

Therefore, in the present study, the researchers proposed to identify dysregulated modules and genes between PO patients and normal controls based on systemic module inference and attract method. Firstly, PPI data were prepared on the basis of the Search Tool for the Retrieval of Interacting Genes/Proteins (STRING) database and gene expression data of PO. Subsequently, attracted modules were explored from PPI networks by clique-merging algorithm and module correlation density (MCD) analyses. Ultimately, dysregulated modules between PO and normal condition were determined utilizing attract method from attracted modules, and genes in the dysregulated modules were defined as dysregulated genes. The results might provide potential biomarkers for detection and therapy of PO, and gain an insight to reveal molecular mechanism underlying this disease.

METHODOLOGY

Collecting PPI Data

From a biological perspective view, genes are inclined to interact with each other in complex disease rather than independent entities (Bi et al. 2015). An effective way to uncover the underlying biology from such co-operated genes is to investigate their interactions. Consequently, the researchers acquired all human PPIs from the STRING database (http://string-db.org) (Szklarczyk et al. 2014). A total of 16,730 genes and 1,048,576 interactions were obtained. Based on them, the researchers removed interactions without expression values or duplicated self-loops, and discarded those of score <0.2. Note that a score was given to each interaction by the STRING database. In result, 7,996 genes and 48,778 interactions were retained.

For purpose of making these interactions more reliable and correlated to PO, we took their intersections with PO dataset with accessing number of E-MEXP-1618 (Reppe et al. 2010) downloaded from the ArrayExpress database (http://www.ebi.ac.uk/arrayexpress/). The dataset presented on A-AFFY-44-Affymetrix GeneChip Human Genome U133 Plus 2.0 Platform, and comprised 39 normal controls and 45 PO samples. Standard corrections and normalizations were conducted on the data to control its quality (Irizarry et al. 2003; Bolstad et al. 2003; Bolstad 2013). After eliminating duplicated probes by feature filter method (Neuda et al. 2012) and converting probes into gene symbols through the annotate package (Zhu et al. 2010), 20,545 genes were detected in the gene expression data. Only interactions with two nodes both belonged to the gene expression data were reserved. Ultimately, the PPI data with 7,953 genes and 48,778 interactions were identified for further exploitation in this study. We should notice that the expression levels for genes in PO patients and normal controls were different, and thus the PPI data for the two conditions also were different.

Identifying Attracted Modules

In this section, the identification of attracted modules was mainly divided into three parts. Based on the PPI data as a backbone and SCC algorithm, the researchers inferred two tissue condition-specific PPI networks, one for normal and one for PO. Next, modules were extracted from the two conditional networks adopting a maximal clique-merging approach. Attracted modules were identified by matching normal and PO modules in gene compositions.

Inferring Normal and PO PPI Network

Among the PPI data in normal and PO condition, a number of false positive or non-effective interactions might be presented. Hence the researchers implemented a common used algorithm, Spearman correlation coefficient (SCC), to reweight these interactions and construct the specific PPI network respectively. Herein, SCC is a measure of correlation between two variables, giving a value between -1 and +1 inclusive (Szmidt and Kacprzyk 2010). If S(i, j) had a positive value, there was a positive linear correlation between the pair of genes. Besides, for a PPI between i and j, the absolute SCC value was denoted as its weight value. Only the interactions with their P <0.05 were reserved, and inputted

them to the Cytoscape to visualize the networks. Cytoscape is an open source software project for integrating biomolecular interactions with high-throughput expression data and other molecular states into a unified conceptual network (Shannon et al. 2003). Consequently, the researchers obtained the PPI network for normal controls and PO patients, respectively.

Extracting Modules from the Networks

The identification of modules was accomplished based on the clique-merging algorithm (Liu et al. 2009; Srihari and Leong 2013). Firstly, the maximal cliques were extracted from the PPI networks by a fast depth-first search with pruning-based algorithm (Tomita et al. 2006). Secondly, a weighted density was assigned to each clique, and these cliques were ranked in non-increasing order of their weighted densities. Ultimately, the researchers went through this ordered list repeatedly merging highly overlapping cliques to build modules. In particular, for any clique C, we repeatedly searched for a clique C' such that the overlap $|C \cap C'|/|C'| \geq \delta$, where $\delta = 0.5$ was a predefined threshold for overlapping (Srihari and Ragan 2013). If such a C' was found, the weighted inter-connectivity Iw between C and C' was computed step further. If Iw (C, C') $\geq \delta$, then C' was merged into C forming a module, else C' was discarded. In results, the researchers gained the modules extracted from the PPI networks for normal and PO conditions separately.

Comparing Modules Across Conditions

For purpose of comparing modules across PO condition and normal controls, MCD for each module under special condition was calculated as follow:

$$MCD = \frac{\sum_{i,j \in s} S((i,j), M)}{|S| * (|S| - 1)}$$

Of which M was a similarity graph to perform a maximum weight bipartite matching (Gabow 1976). Suppose that d_{PO} stood for MCD of a module in PO and dNormal represented MCD for normal controls, the absolute difference of MCD, ? = $|d_{PO} - d_{Normal}|$, was denoted as the index to choose similar or same module pairs across the two conditions. Each module in this kind of module pair was considered to be an attracted module for PO.

Investigating Dysregulated Modules

Using attracted modules detected above, an attract method, which is a knowledge driven analytical approach for identifying and annotating the gene-sets (Mar et al. 2011), was utilized to investigate dysregulated modules between PO patients and normal controls. It could be summarized the determination of dysregulated modules that discriminated the most strongly between cell types or experimental groups of interest (Mar 2011). Particularly, under GSEA-ANOVA, the researchers fitted an ANOVA model to each gene where a gene's expression was modeled by a single factor representing the cell types as distinct levels of this class. From the ANOVA model, the F-statistic for gene i was calculated:

Where MSSi represented the mean treatment sum of squares, and captured the amount of variation due to the cell type group-specific effects:

$$MSS_i = \frac{1}{K-1} \sum_{k=1}^{K} r_k \left[u_{.k}^{(i)} - u_{..}^{(i)}\right]^2$$

And RSSi stood for the residual sum of squares:

$$F^{(i)} = \frac{MSS_i}{RSS_i}$$

$$RSS_i = \frac{1}{N-K} \sum_{k=1}^{K} \sum_{v=1}^{rv} \left[u_{vk}^{(i)} - u_{..}^{(i)}\right]^2$$

Of which v represented corresponding expression value in each replicate sample; rk for each cell type k = 1, …, K; u stood for the mixed effect model; N meant the total number of samples. Large values of the F-statistic indicated a strong association whereas a small F-statistic suggested that the gene demonstrated minimal cell type-specific expression changes. In order to make the F-statistic more confidence, we selected T test to correct the log2-transformed F-statistics and obtain P value for each potentially shared module originated from synexpression groups. Adjusting their P values on the basis of false discovery rate (FDR) (Benjamini and Hochberg 1995), the researchers defined the modules with $P < 0.05$ as dysregulated modules between PO and normal condition.

RESULTS

Attracted Modules

In the present study, the researchers employed gene expression data and PPI data to pro-

vide the backbone for PPI networks of PO and normal condition. In addition, SCC method was applied to select interactions with $P < 0.05$ for constructing the two specific PPI networks respectively, and assign a weight value to each edge in them. In result, we obtained the PPI networks for PO and normal controls with equal amount of 7,953 nodes and 48,778 interactions. As shown in Figure 1, the researchers found that a major number of interactions ranged from 0 to 0.2 both for PO condition and normal condition. But from an overall perspective of the two curves, their weight distributions had clear difference, especially in the section of 0.1 ~ 0.4. Nevertheless, these results couldn't offer effective information for clinical treatment and molecular mechanism, while too large scale of PPI networks might be too generic. And thus the researchers focused on detecting sub-networks or modules that extracted from the PPI networks.

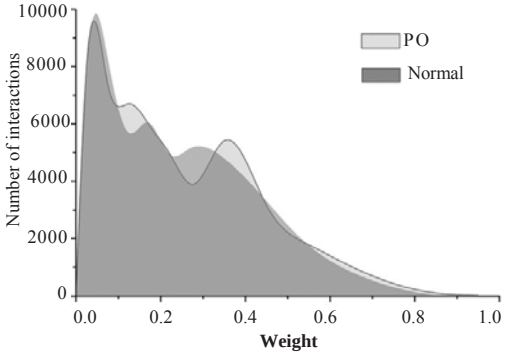

Fig. 1 Weight distribution of interactions in protein-protein interaction (PPI) networks for postmenopausal osteoporosis (PO) condition and normal controls.
Source: Author

Utilizing the fast depth-first method in clique algorithm, a total of 10,089 and 8,620 maximal cliques were explored from the PPI networks of PO samples and normal controls, respectively. After removing maximal cliques with too small genes (Node number < 4), 2,172 and 1,017 were reserved for the two conditions separately. Subsequently, a weighted density was assigned to each maximal clique, in particular, the statistical chart for cliques of their node numbers and densities were illustrated in Figure 2. The results uncovered that with the increase of node number, the amount of cliques was decreased. In detail, the most node number in normal condition

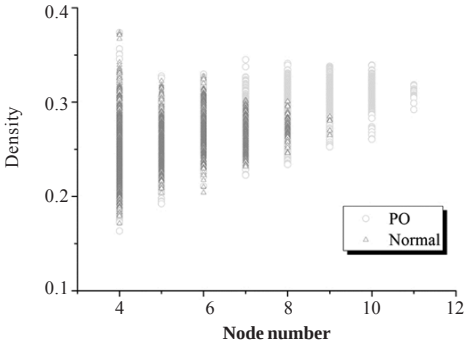

Fig. 2. The statistical chart for cliques of their node numbers and densities.
Source: Author

was 9, while that of PO condition was 11. Besides, a maximal clique of PO possessed the highest density compared with normal condition. In addition, maximal cliques with high overlaps (? ? 0.5) were merged together to form a module, and the researchers obtained 11 modules for PO condition (Table 1) and 6 modules for normal condition (Table 2). For each module, the number of genes enriched in it was denoted as its count value. Module 4 of PO had the highest count of 10.

When comparing the modules across PO and normal condition based on the computation of absolute MCD difference, the researchers discovered that two pairs of matched modules had the same gene compositions coincidently. They were Module 5 of PO versus Module 2 of normal, and Module 8 of PO versus Module 6 of normal. In addition, each module pair was considered to be an attracted module for PO, and hence two attracted modules were gained, Module 1 and Module 2.

Dysregulated Modules

After identifying attracted modules for PO patients, further study should be conducted focusing on investigating significantly dysregulated modules and genes between PO and normal controls. In this work, GSEA-ANOVA model in attract method was implemented, which also gave us a way to gauge genes that informative for a particular set of cell types. Supposing that each attracted module was an attractor, the dysregulated modules were investigated according to the F-statistic significance analysis. With the thresholding of $P < 0.05$, the researchers could gain the dysregulated modules for PO, and genes

Table 1: Differentially methylated genes (DMGs)

Rank	*DMG*	*P value*	*Rank*	*DMG*	*P value*
1	ERCC3	4.48E-59	24	VCL	5.46E-47
2	TNFRSF9	5.22E-57	25	MYEOV	6.56E-47
3	HRH4	1.52E-56	26	CSNK1D	1.12E-46
4	PVT1	9.40E-56	27	ZFP36L1	1.21E-46
5	FOXP1	2.96E-55	28	WDR45B	1.59E-46
6	ZGPAT	5.20E-54	29	SORCS2	1.28E-42
7	RCAN3	2.91E-53	30	RUNX3	8.15E-40
8	IQCB1	4.53E-53	31	ATXN7	1.55E-38
9	SPTBN1	6.21E-53	32	TCF12	7.88E-28
10	PYURF	2.67E-52	33	FYCO1	1.91E-21
11	WDR49	2.71E-52	34	WDR20	2.85E-20
12	VRK2	1.78E-51	35	PDCD1	6.33E-14
13	GMDS	5.64E-51	36	CD1C	6.62E-14
14	LOC256880	6.33E-51	37	C6orf10	1.06E-13
15	PTEN	2.50E-50	38	MRGPRG-AS1	3.22E-13
16	DOCK2	3.39E-50	39	TMEM198	9.26E-13
17	TMCO3	7.56E-50	40	HLA-DQB1	2.85E-12
18	TRIM27	2.98E-49	41	MAGI2-AS3	8.17E-12
19	DRGX	3.32E-49	42	HLA-DRB6	2.19E-10
20	LINC00520	3.42E-49	43	DNAJB6	3.47E-10
21	RAD51B	5.56E-49	44	ASCL2	2.48E-09
22	FAM120B	2.23E-48	45	HLA-DRB5	7.44E-08
23	ADAMTS14	2.28E-48	46		

Table 2: Significant KEGG pathways with P < 0.05

ID	*Pathway*	*P value*
PATH:hsa04514	Cell adhesion molecules (CAMs)	1.71E-03
PATH:hsa04672	Intestinal immune network for IgA production	2.56E-03
PATH:hsa05310	Asthma	2.72E-03
PATH:hsa05320	Autoimmune thyroid disease	3.13E-03
PATH:hsa05330	Allograft rejection	3.43E-03
PATH:hsa05332	Graft-versus-host disease	4.07E-03
PATH:hsa05416	Viral myocarditis	4.94E-03
PATH:hsa04940	Type I diabetes mellitus	5.50E-03
PATH:hsa05150	Staphylococcus aureus infection	6.09E-03
PATH:hsa05321	Inflammatiory bowel disease (IBD)	7.58E-03

enriched in dysregulated modules were regarded as dysregulated genes. The results showed that two dysregulated modules were identified (Module 1 and Module 2). Specifically, Module 1 with P = 1.25E-03 was comprised of 6 dysregulated genes (ASF1B, CDC45, MCM5, RNASEH2A, MCM4 and MCM7). Whereas Module 2 (P = 3.18E-04) involved 7 dysregulated genes (LIG1, MCM5, MCM3, CDC45, MCM4, CDC6 and FEN1). Interestingly, CDC45, MCM4 and MCM5 were deposited in both of the two modules. Except the common ones, 10 dysregulated genes were detected totally.

What's more, the networks for Module 1 and Module 2 were described in Figure 3. All dysregulated genes worked or interacted with the other genes of modules. There were 15 interactions among 6 nodes for Module 1, and 21 interactions involved in 7 nodes for Module 2. The dysregulated module and genes might play more significant role than the other modules and genes in the progression of PO and be potential biomarkers in the target treatment.

DISCUSSION

It has been revealed that the most significant genes and modules obtained from different studies for a particular disease are typically inconsistent (Ein-Dor et al. 2005). To overcome this problem, one could evaluate pathogenic genes or modules for disease-association using a network strategy (Zhang et al. 2013). For instance, Magger et al. (2012) combined PPI and gene expression data to construct tissue-specific PPI net-

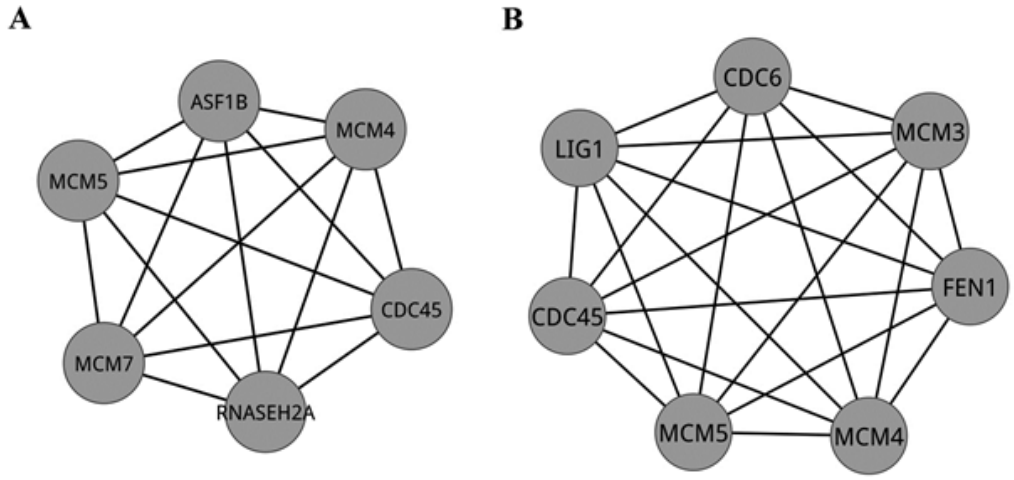

Fig. 3. Network for dysregulated modules. A: Module 1; B: Module 2. Nodes represented core genes, and edges were the interactions among any two genes.

works and used them to prioritize disease genes. Beyond straightforward scoring genes in the complex network, it is crucial to study the behavior of modules across specific conditions in a controlled manner to understand the modus operandi of disease mechanisms and to implicate novel genes (Srihari and Ragan 2013), since some of important genes may not be identifiable through their own behavior, but their changes are quantifiable when considered in conjunction with other genes as modules. What is required, therefore, is a systematic tracking gene and module behavior across specific conditions in a controlled manner (Wang et al. 2015).

In the present paper, the researchers investigated dysregulated modules and genes between PO patients and normal controls based on the systemic module inference and attract method. The results showed that a total of 2 dysregulated modules (Module 1 and Module 2) and 10 dysregulated genes (ASF1B, CDC45, MCM5, RNASEH2A, MCM4 MCM7, LIG1, MCM3, CDC6 and FEN1) were obtained for PO. In particular, CDC45, MCM4 and MCM5 were the common genes of the two modules. Among dysregulated genes, 2 (CDC45 and CDC6) belonged to the cell division cycle (CDC) family, and 4 ones (MCM3, MCM4, MCM5 and MCM7) were attributed to the minichromosome maintenance complexes (MCMs).

CDC45, an essential gene required to initiation of DNA replication in eukaryotes, is a member of the highly conserved multi-proteins CMG (CDC45/MCM2-7/GINS) that is thought to function as a replicative DNA helicase (Ilves et al. 2010). It can directly interact with all MCM2-7 genes, GINS, and other replication proteins. The MCM2-7 helicase complex is activated when associated with CDC45 and GINS and that this activation involves multiple aspects of the unwinding process, including enhanced the ATP hydrolysis and better DNA substrate recognition. At the same time, CDC45 and GINS allosterically form a scaffold on the MCM ring that assists in the proper coordination of different subunits in the MCM2-7 motor, thus leading to its efficient unwinding of DNA strands (Costa et al. 2011). Ilves et al. (2010) had demonstrated that MCM2-7 core enzyme provides the necessary activation step for the replicative helicase and the concomitant initiation of DNA synthesis, and provided evidence that the MCM4 was a distinct and important target of regulatory cell-cycle-dependent kinases and the main binding partner for the GINS. As a consequence, dysregulated gene MCM3, MCM4, MCM5 and MCM7 and their enriched modules were very significant for molecular biological activities in human beings, and their dysregulations perhaps led to certain disease, such as PO.

What's more, a considerable portion of CDC45 localizes in a region other than the DNA replication forks in nuclei or it localizes on the replication forks but it is not fractionated with

the fork proteins owing to its tight association with presumably nuclear scaffolds (Takaya et al. 2013). Besides, the level of CDC45 recovered from Triton-insoluble -containing fraction was peaked at middle of S phase in synchronized HeLa cells (Takaya et al. 2013), which indicated its significance for cell divisions of women. Beyond that, CDC6 functions as a regulator at the early steps of DNA replication, localizes in cell nucleus during cell cyle G1, but translocates to the cytoplasm at the start of S phase (Sideridou et al. 2011). Its subcellular translocation during cell cycle is regulated through its phosphorylation by CDKS. CDC6 could also interacted with MCM2-7 and formed an complex through a multistep reaction to serve as a platform for MCM double-hexamer assembly (Fernández-Cid et al. 2013). Consequently, the researchers might infer that CDC45, CDC6 and their enriched modules played an important role in DNA replications and cell cycle related activities of PO patients.

CONCLUSION

In conclusion, the researchers have identified 2 dysregulated modules and 10 dysregulated genes for PO utilizing module inference and attract method. The findings may provide potential biomarkers for prevention and treatment of PO progression, and give great insights to revealing molecular mechanism underlying the disease.

RECOMMENDATIONS

Whereas, how these dysregulated modules interacted with each other is still unclear, and the validations should be carried out in future.

REFERENCES

Benjamini Y, Hochberg Y 1995. Controlling the false discovery rate: A practical and powerful approach to multiple testing. *Journal of the Royal Statistical Society: Series B (Methodological),* 57(1): 289-300.

Bi D, Hao N, Liu S, Que X, Ding K 2015. Gene expression patterns combined with network analysis identify hub genes associated with bladder cancer. *Computational Biology and Chemistry,* 56: 71-83.

Bolstad BM, Irizarry RA, Astrand M, Speed TP 2013. A comparison of normalization methods for high density oligonucleotide array data based on variance and bias. *Bioinformatics,* 19: 185-193.

Cosman F, De Beur S, LeBoff M, Lewiecki E, Tanner B, Randall S, Lindsay R 2014. Clinician's guide to prevention and treatment of osteoporosis. *Osteoporosis International,* 25: 2359-2381.

Costa A, Ilves I, Tamberg N, Petojevic T, Nogales E, Botchan MR, Berger JM 2011. The structural basis for MCM2-7 helicase activation by GINS and Cdc45. *Nature Structural and Molecular Biology,* 18: 471-477.

Delmas PD 2008. Clinical potential of RANKL inhibition for the management of postmenopausal osteoporosis and other metabolic bone diseases. *Journal of Clinical Densitometry,* 11: 325-338.

Ein-Dor L, Kela I, Getz G, Givol D, Domany E 2005. Outcome signature genes in breast cancer: Is there a unique set? *Bioinformatics,* 21: 171-178.

Fernández-Cid A, Riera A, Tognetti S, Herrera MC, Samel S, Evrin C, Winkler C, Gardenal E, Uhle S, Speck C 2013. An ORC/Cdc6/MCM2-7 complex is formed in a multistep reaction to serve as a platform for MCM double-hexamer assembly. *Molecular Cell,* 50: 577-588.

Gabow HN 1976. An efficient implementation of Edmonds' algorithm for maximum matching on graphs. *Journal of the ACM (JACM),* 23: 221-234.

Ilves I, Petojevic T, Pesavento JJ, Botchan MR 2010. Activation of the MCM2-7 helicase by association with Cdc45 and GINS proteins. *Molecular Cell,* 37: 247-258.

Irizarry RA, Bolstad BM, Collin F, Cope LM, Hobbs B, Speed TP 2003. Summaries of affymetrix genechip probe level data. *Nucleic Acids Research,* 31: e15.

Jordán F, Nguyen TP, Liu WC 2012. Studying protein-protein interaction networks: A systems view on diseases. *Briefings in Functional Genomics,* 11: 497-504.

Liu G, Wong L, Chua HN 2009. Complex discovery from weighted PPI networks. *Bioinformatics,* 25: 1891-1897.

Liu Y, Koyutürk M, Barnholtz-Sloan JS, Chance MR 2012a. Gene interaction enrichment and network analysis to identify dysregulated pathways and their interactions in complex diseases. *BMC Systems Biology,* 6: 65.

Liu ZP, Wang Y, Zhang XS, Chen L 2012b. Network-based analysis of complex diseases. *IET Systems Biology,* 6: 22-33.

Magger O, Waldman YY, Ruppin E, Sharan R 2012. Enhancing the prioritization of disease-causing genes through tissue specific protein interaction networks. *PLoS Computational Biology,* 8: e1002690.

Manocha A, Srivastava LM, Bhargava S 2017. Lead as a risk factor for osteoporosis in post-menopausal women. *Indian J Clin Biochem,* 32: 261-265.

Mar J 2011. Methods to Find the Gene Expression Modules that Represent the Drivers of Kauffman's Attractor Landscape. Version 1.18.0

Mar JC, Matigian NA, Quackenbush J, Wells CA 2011. attract: A method for identifying core pathways that define cellular phenotypes. *Plos One*, 6(10): e25445.

Nueda M, Ferrer A , Conesa A 2012. ARSyN: A method for the identification and removal of systematic noise in multifactorial time course microarray experiments. *Biostatistics,* 13: 553-566.

Orwoll E, Vanderschueren D, Boonen S 2013. Osteoporosis in men. Epidemiology, pathophysiology, and clinical characterization. In: *Elsevier Inc Osteoporosis,* Two-Volume Set, pp. 103-149.

Ozsoy AZ, Karakus N, Tural S, Yigit S, Kara N, Alayli G, Tumer MK, Kuru O 2017. Influence of the MIF polymorphism -173G > C on Turkish postmenopausal women with osteoporosis. *Z Rheumatol,* Suppl 7:1-4.

Reppe S, Refvem H, Gautvik VT, Olstad OK, Høvring PI, Reinholt FP, Holden M, Frigessi A, Jemtland R, Gautvik KM 2010. Eight genes are highly associated with BMD variation in postmenopausal Caucasian women. *Bone,* 46: 604-612.

Shannon P, Markiel A, Ozier O, Baliga NS, Wang JT, Ramage D, Amin N, Schwikowski B, Ideker T 2003. Cytoscape: A software environment for integrated models of biomolecular interaction networks. *Genome Research,* 13: 2498-2504.

Sideridou M, Zakopoulou R, Evangelou K, Liontos M, Kotsinas A, Rampakakis E, Gagos S, Kahata K, Grabusic K, Gkouskou K 2011. Cdc6 expression represses E-cadherin transcription and activates adjacent replication origins. *Journal of Cell Biology,* 195: 1123-1140.

Srihari S, Leong HW 2013. A survey of computational methods for protein complex prediction from protein interaction networks. *Journal of Bioinformatics and Computational Biology,* 11(2): 1230002.

Srihari S, Ragan MA 2013. Systematic tracking of dysregulated modules identifies novel genes in cancer. *Bioinformatics,* 29(12): 1553-1561.

Stuss M, Rieske P, Ceg³owska A, Stêpieñ-K³os W, Liberski PP, Brzeziañska E, Sewerynek E 2013. Assessment of OPG/RANK/RANKL gene expression levels in peripheral blood mononuclear cells (PBMC) after treatment with strontium ranelate and ibandronate in patients with postmenopausal osteoporosis. *The Journal of Clinical Endocrinology and Metabolism,* 98: E1007-E1011.

Sun SY, Liu ZP, Zeng T, Wang Y, Chen L 2013. Spatiotemporal analysis of type 2 diabetes mellitus based on differential expression networks. *Sci Rep,* 3: 2268.

Svedbom A, Ivergård M, Hernlund E, Rizzoli R, Kanis J 2014. Epidemiology and economic burden of osteoporosis in Switzerland. *Archives of Osteoporosis,* 9: 1-8.

Szklarczyk D, Franceschini A, Wyder S, Forslund K, Heller D, Huerta-Cepas J, Simonovic M, Roth A, Santos A, Tsafou KP 2014. STRING v10: Protein–protein interaction networks, integrated over the tree of life. *Nucleic Acids Research,* 43(Database Issue): D447-D452.

Szmidt E, Kacprzyk J 2010. The Spearman Rank Correlation Coefficient between Intuitionistic Fuzzy Sets. *In: IEEE International Conference on Intelligent Systems,* 7-9 July, University of Westminster, London, UK, pp. 276-280.

Takaya J, Kusunoki S, Ishimi Y 2013. Protein interaction and cellular localization of human CDC45. *The Journal of Biochemistry,* 153: 381-388.

Tomita E, Tanaka A, Takahashi H 2006. The worst-case time complexity for generating all maximal cliques and computational experiments. *Theoretical Computer Science,* 363: 28-42.

Tsai JN, Uihlein AV, Lee H, Kumbhani R, Siwilasackman E, Mckay EA, Burnettbowie SA, Neer RM, Leder BZ 2013. Teriparatide and denosumab, alone or combined, in women with postmenopausal osteoporosis: The DATA study randomised trial. *Lancet,* 382: 50-56.

Unni S, Yao Y, Milne N, Gunning K, Curtis JR, Lafleur J 2015. An evaluation of clinical risk factors for estimating fracture risk in postmenopausal osteoporosis using an electronic medical record database. *Osteoporosis International,* 26: 581-587.

Vinayagam A, Zirin J, Roesel C, Hu Y, Yilmazel B, Samsonova AA, Neumüller RA, Mohr SE, Perrimon N 2014. Integrating protein-protein interaction networks with phenotypes reveals signs of interactions. *Nature Methods,* 119: 6399-6420.

Wang SM, Sun ZQ, Li HY, Wang J, Liu QY 2015. Temporal identification of dysregulated genes and pathways in clear cell renal cell carcinoma based on systematic tracking of disrupted modules. *Computational and Mathematical Methods in Medicine,* Article 1D313740, 11 pages. http://dx.dir.org/10.1155/2015/313740.

Wang Y, Li L, Moore BT, Peng XH, Fang X, Lappe JM, Recker RR, Xiao P 2012. MiR-133a in human circulating monocytes: A potential biomarker associated with postmenopausal osteoporosis. *PLoS ONE,* 7: 282.

Zhang L, Li S, Hao C, Hong G, Zou J, Zhang Y, Li P, Guo Z 2013. Extracting a few functionally reproducible biomarkers to build robust subnetwork-based classifiers for the diagnosis of cancer. *Gene,* 526: 232-238.

Zhu LJ, Gazin C, Lawson ND, Pagès H, Lin SM, Lapointe DS, Green MR 2010. ChIPpeakAnno: A bioconductor package to annotate ChIP-seq and ChIP-chip data. *BMC Bioinformatics,* 11: 237.

Paper received for publication on March 2018
Paper accepted for publication on May 2018